PERGAMON

International Journal of Heat and Mass Transfer 45 (2002) 2387–2396

International Journal of HEAT and MASS TRANSFER

www.elsevier.com/locate/ijhmt

Numerical visualization of mass and heat transport for mixed convective heat transfer by streamline and heatline

Qi-Hong Deng, Guang-Fa Tang *

College of Civil Engineering, Hunan University, Changsha, Hunan 410082, China

Received 15 May 2001

Abstract

Based on the method we suggested in a previous paper [Int. J. Heat Mass Transfer 45 (2002) pp. 2373–2385], the present work is to investigate the mixed convection problem. A two-dimensional, steady, laminar displacement ventilation model is adopted here for the interaction between the buoyancy driven natural convection and the external forced convection is important to achieve the goal of ventilation effectiveness. The solution is determined by the non-dimensional parameters Gr and Gr/Re^2, the influences of which on the resulting heat and fluid flow are discussed. To optimize the ventilation system, different outlet locations are investigated. Results and comparisons show that the displacement ventilation guarantees a high indoor air quality (IAQ) and is therefore a desired air-conditioning system.

1. Introduction

As a counterpart to [1], this paper deals with the heatline visualization of heat transfer for mixed convection for a new application. The present study is initiated by the research on the complicated flow patterns occurring in the displacement ventilation (air-conditioning) system [2,3].

Traditional air-conditioning system in office supplies the fresh and cold air from above and releases the contaminated and warm air through the outlet below, as schematically shown in Fig. 1, but with the flow direction reversed. This system prevailed in the past for being easily designed and installed, and could meet the people's basic cooling demand. Recently, with the development of the office automation, the heat sources or devices (such as computers and duplicating machine, etc.) are increasing, which challenges to the traditional air-conditioning system. Meanwhile, with the living standard increasing, people's have turn attention to the indoor air quality (IAQ), which has been proved much related to the people's health and work efficiency [4–7]. The buildings equipped with the air-conditioning system, however, cannot adapt to the new advance and are considered as sick buildings.

To improve the IAQ and to create a healthy and comfortable environment, a new air-conditioning system, displacement ventilation, has been proposed, which spread wide quickly and received much attention during the last decade [8,9]. For the typical displacement ventilation system is schematically shown in Fig. 1, a heat source lies on the left half of the floor and a working zone occupies the right lower part of the room. The conditioned cold air is supplied from a low side wall diffuser and spreads over the floor. When the cold air meets the heat source, convection plume is generated, the warmed and polluted air goes upwards to the ceiling where it exits through the exhaust. As expected, the fresh cold air is first conveyed through the people's working zone, resulting in a higher IAQ. The system will be energy saving because the required amount of fresh cold air and cool loads can be reduced.

In displacement ventilation, both natural and forced convection must be taken into account. The interaction between the two convective flows is important to achieve the effectiveness of ventilation. Visualizing the

* Corresponding author. Tel.: +86-731-882-2760; fax: +86-731-882-1342.

E-mail address: gftang@mail.hunu.edu.cn (G.-F. Tang).

0017-9310/02/$ - see front matter
PII: S0017-9310(01)00317-9

Nomenclature

g	gravitational acceleration
Gr	Grashof number ($Gr = g\beta\Delta TL^3/\nu^2$)
h	local heat transfer coefficient
$\bar{h}$	average heat transfer coefficient
H	dimensionless heat function
k	thermal conductivity
L	length of enclosure
n	outside normal to the boundary surface
$\overline{Nu}$	average Nusselt number
p	pressure
P	dimensionless pressure ($P = (p/\rho u_c^2)$)
Pr	Prandtl number ($Pr = \nu/\alpha$)
q_s''	heat flux over the surface of heat source
Re	Reynolds number ($Re = u_i L/\nu$)
T	temperature
u, v	Cartesian velocities
U, V	dimensionless Cartesian velocities ($(U, V) = (u, v)/u_c$)
u_c	characteristic velocity ($u_c = \sqrt{g\beta\Delta TL}$)
x, y	Cartesian coordinates
X, Y	dimensionless Cartesian coordinates ($(X, Y) = (x, y)/L$)

Greek symbols

α	fluid thermal diffusivity
β	fluid thermal expansion coefficient
ν	fluid kinematic viscosity
ρ	fluid density
θ	dimensionless temperature ($\theta = (T - T_i)/\Delta T$)
ΔT	temperature scale ($\Delta T = q_s'' L/k$)
ψ	dimensionless stream function

Subscripts

i	inlet
max	maximum
s	heat source

processes may provide a new means to understand the philosophy. The objective of this paper is to analyze the fluid flow and heat transfer characteristics of the displacement ventilation using the method of streamline and heatline. We will investigate the effects of the governing parameters Gr and Gr/Re^2, then the influence of the location of the outlet and discuss the results as compared to the traditional air-conditioning system. The methodology developed and the results obtained will be useful also for other mixed convection applications such as the thermal management of electronics [10].

2. Analysis

The physical model of displacement ventilation considered here is schematically shown in Fig. 1. It is a square room, with sides of length L, whose walls are maintained adiabatic except for the left half of the floor where lies a heat source generating a uniform heat flux q_s''. The fresh cold air, with mean velocity u_i and temperature T_i, is supplied from the opening at the lower part of the side wall with size of $L/8$. An outlet of the same size as the inlet exhausts the warm air from the top side wall. The gravitational acceleration acts parallel to the side walls. All fluid properties are assumed constant and taken at the reference inlet temperature, except for density in buoyancy term that follows the Boussinesq approximation.

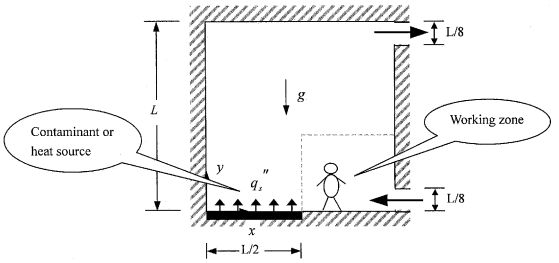

Fig. 1. Schematic flow configuration of displacement ventilation system.

2.1. Governing equations

A two-dimensional, steady state, incompressible laminar flow model is considered in the present study. The governing equations of mass, momentum and energy conservation can be written, in non-dimensional conservative form, as follows:

$$\frac{\partial U}{\partial X} + \frac{\partial V}{\partial Y} = 0, \tag{1}$$

$$\frac{\partial}{\partial X}(UU) + \frac{\partial}{\partial Y}(VU) = -\frac{\partial P}{\partial X} + \frac{1}{\sqrt{Gr}}\nabla^2 U, \tag{2}$$

$$\frac{\partial}{\partial X}(UV) + \frac{\partial}{\partial Y}(VV) = -\frac{\partial P}{\partial Y} + \frac{1}{\sqrt{Gr}}\nabla^2 V + \theta, \tag{3}$$

$$\frac{\partial}{\partial X}(U\theta) + \frac{\partial}{\partial Y}(V\theta) = \frac{1}{Pr\sqrt{Gr}}\nabla^2\theta. \tag{4}$$

The above governing equations are non-dimensionalized using the following scales:

Table 1
The comparison of the predicted average Nusselt numbers at different grid distribution for the case of $Gr = 10^5$ and $Gr/Re^2 = 1$

	20×20	30×30	40×40	50×50	60×60
$\overline{Nu}$	5.28	5.72	5.92	6.02	6.06

Velocity scale: $u_c = \sqrt{g\beta\Delta TL}$; length scale: L; temperature scale: $\Delta T = q''_s L/k$.

Accordingly, the non-dimensional variables are defined as:

$$(X, Y) = (x, y)/L, \quad (U, V) = (u, v)/u_c,$$
$$\theta = (T - T_i)/\Delta T, \quad P = p/\rho u_c^2.$$

The non-dimensional parameters that appear in the formulation are the Prandtl number ($Pr = \nu/\alpha$), the Grashof number ($Gr = g\beta\Delta TL^3/\nu^2$) and the Reynolds number ($Re = u_i L/\nu$). Note that although the Reynolds number does not appear in the equations explicitly, it does appear in the boundary conditions in the expression for the non-dimensional inlet velocity as $Re/\sqrt{Gr}$. The ratio Gr/Re^2 indicates the relative strength of the natural and forced convection mechanisms. For the present work, air is considered as the fluid medium, and the Prandtl number is constant ($Pr = 0.71$). Therefore, attention is focused on the effect of Gr and Gr/Re^2 on the heat transfer and flow structures of the system.

2.2. Boundary conditions

On solid walls: No-slip condition is applied for velocities, i.e., $U = V = 0$. All thermal boundary conditions are adiabatic ($\partial\theta/\partial n = 0$), except for those of heat source where $\partial\theta/\partial n = -1$.

$$\text{At inlet}: \quad U = \frac{u_i}{u_c} = -\frac{Re}{\sqrt{Gr}}, \quad V = 0, \quad \theta = 0. \tag{5}$$

$$\text{At outlet}: \quad U = \frac{Re}{\sqrt{Gr}}, \quad V = 0, \quad \partial\theta/\partial n = 0. \tag{6}$$

2.3. Numerical simulation

The methodology proposed for analyzing natural convection in our previous paper [1] is employed here to investigated the mixed convection, with a slightly code modification to reflect the coefficient variations in the governing equations.

In order to ensure the grid-independence solutions, a series of trial calculation were conducted for different grid distributions: 30×30, 40×40, 50×50, 60×60. Table 1 presents a comparison of the predicted average Nusselt numbers, using different grid arrangements, for the case of $Gr = 10^5$ and $Gr/Re^2 = 1$. It was observed that difference between the result of the grid 50×50 and that of the grid 60×60 is less than 0.7%. Consequently, to optimize appropriate grid refinement with computational efficiency, the grid 50×50 was chosen for all the further computations.

The local heat transfer coefficient on the heat source surface is defined in terms of the inlet air temperature T_i as

$$h_x = q''_s/(T_s(x) - T_i), \tag{7}$$

where $T_s(x)$ is the local temperature of the heat source. The average heat transfer coefficient $\bar{h}$ is given as

$$\bar{h} = \frac{1}{L_s}\int_0^{L_s} h_x \, dx, \tag{8}$$

where L_s is the length of the heat source, $L_s = L/2$. The average Nusselt number is obtained using the expression

$$\overline{Nu} = \bar{h}L/k = 2\int_0^{1/2} \frac{1}{\theta_s(X)} \, dX. \tag{9}$$

3. Streamfunction and heatfunction formulation

According to [1], the non-dimensional streamfunction and heatfunction are defined as:

$$-\frac{\partial\psi}{\partial X} = V, \quad \frac{\partial\psi}{\partial Y} = U; \tag{10}$$

$$-\frac{\partial H}{\partial X} = V\theta - \frac{1}{Pr\sqrt{Gr}}\frac{\partial\theta}{\partial Y},$$
$$\frac{\partial H}{\partial Y} = U\theta - \frac{1}{Pr\sqrt{Gr}}\frac{\partial\theta}{\partial X}. \tag{11}$$

Then the corresponding equations are obtained

$$\frac{\partial^2\psi}{\partial X^2} + \frac{\partial^2\psi}{\partial Y^2} + \frac{\partial V}{\partial X} - \frac{\partial U}{\partial Y} = 0, \tag{12}$$

$$\frac{\partial^2 H}{\partial X^2} + \frac{\partial^2 H}{\partial Y^2} + \frac{\partial}{\partial X}(V\theta) - \frac{\partial}{\partial Y}(U\theta) = 0. \tag{13}$$

The boundary conditions of the streamfunction and the heatfunction, for the considered problem, are as follows:

$$\text{At } X = Y = 0: \quad \psi(0,0) = 0, \ H(0,0) = 0; \tag{14}$$

$$\text{At } Y = 0: \quad \psi(X,0) = 0, \quad H(X,0) = \begin{cases} -\int_0^X \frac{1}{Pr\sqrt{Gr}}\, dX, & 0 < X \leqslant 1/2, \\ H(1/2,0), & 1/2 < X \leqslant 1; \end{cases} \tag{15}$$

Table 2
Calculated ranges of Gr and Gr/Re^2

Gr	Gr/Re^2		
	$Re = 100$	$Re = \sqrt{10} \times 100$	$Re = 1000$
10^3	0.1	0.01	0.001
10^4	1	0.1	0.01
10^5	10	1	0.1
10^6	100	10	1

$$\text{At } X = 0: \quad \psi(0, Y) = 0, \quad H(0, Y) = 0; \tag{16}$$

$$\text{At } Y = 0: \quad \psi(X, 1) = 0, \quad H(X, 1) = 0; \tag{17}$$

$$\text{At } X = 1:$$

$$\psi(1, Y) = \begin{cases} -\int_0^Y Re/\sqrt{Gr}\,\mathrm{d}Y, & 0 < Y \leqslant 1/8, \\ \psi(1, 1/8), & 1/8 < Y \leqslant 7/8, \\ \psi(1, 1/8) + \int_0^Y Re/\sqrt{Gr}\,\mathrm{d}Y, & 7/8 < Y \leqslant 1, \end{cases}$$

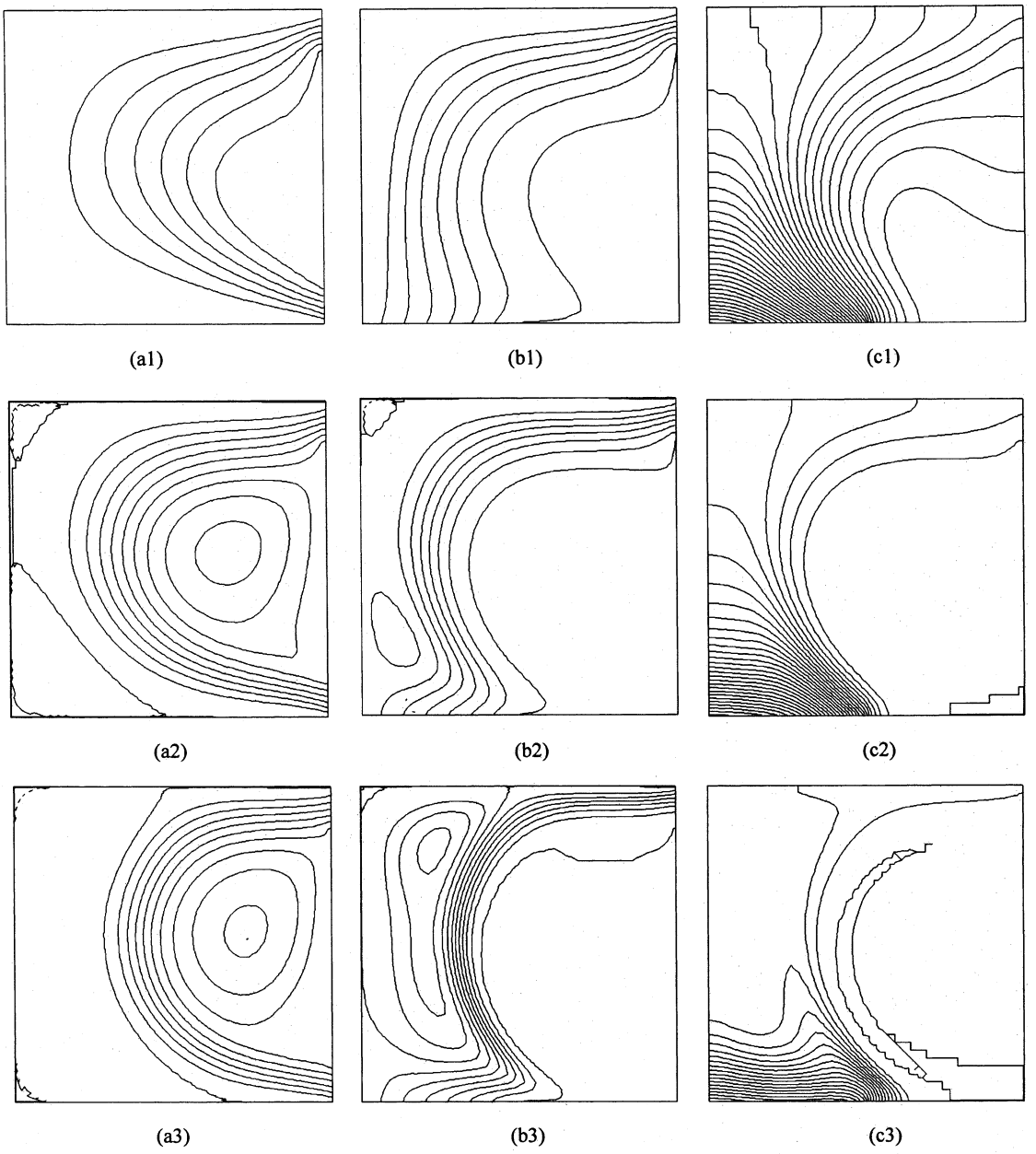

Fig. 2. Streamline (a), heatline (b) and isotherm (c) at $Gr = 10^4$ for different Gr/Re^2: (1) $Gr/Re^2 = 1$; (2) $Gr/Re^2 = 0.1$; (3) $Gr/Re^2 = 0.01$.

$$H(1,Y)=\begin{cases} H(1,0)-\int_0^Y \frac{1}{Pr\sqrt{Gr}}\frac{\partial\theta}{\partial X}\,dY, & 0<Y\leqslant 1/8,\\ H(1,1/8), & 1/8<Y\leqslant 7/8,\\ H(1,1/8)+\int_0^Y Re/\sqrt{Gr}\theta\,dY, & 7/8<Y\leqslant 1. \end{cases} \tag{18}$$

4. Results and discussion

For the laminar governing equations (1)–(4), the steady solution is conditional and determined by the ranges of the non-dimensional parameters Gr and Gr/Re^2. As listed in Table 2, the values of Grashof number cast in the range of 10^3–10^6. For each value of Gr, the ratio Gr/Re^2 varies until the stable solution could not be obtained. It was observed that beyond the critical values, i.e., $Gr \geqslant 10^7$ or $Re \geqslant 3000$, the solution could not be converged. However, the turbulent flow is expected to arise, and a suitable turbulent closure model will be needed to simulate the flow satisfactory, which is beyond the scope of this paper.

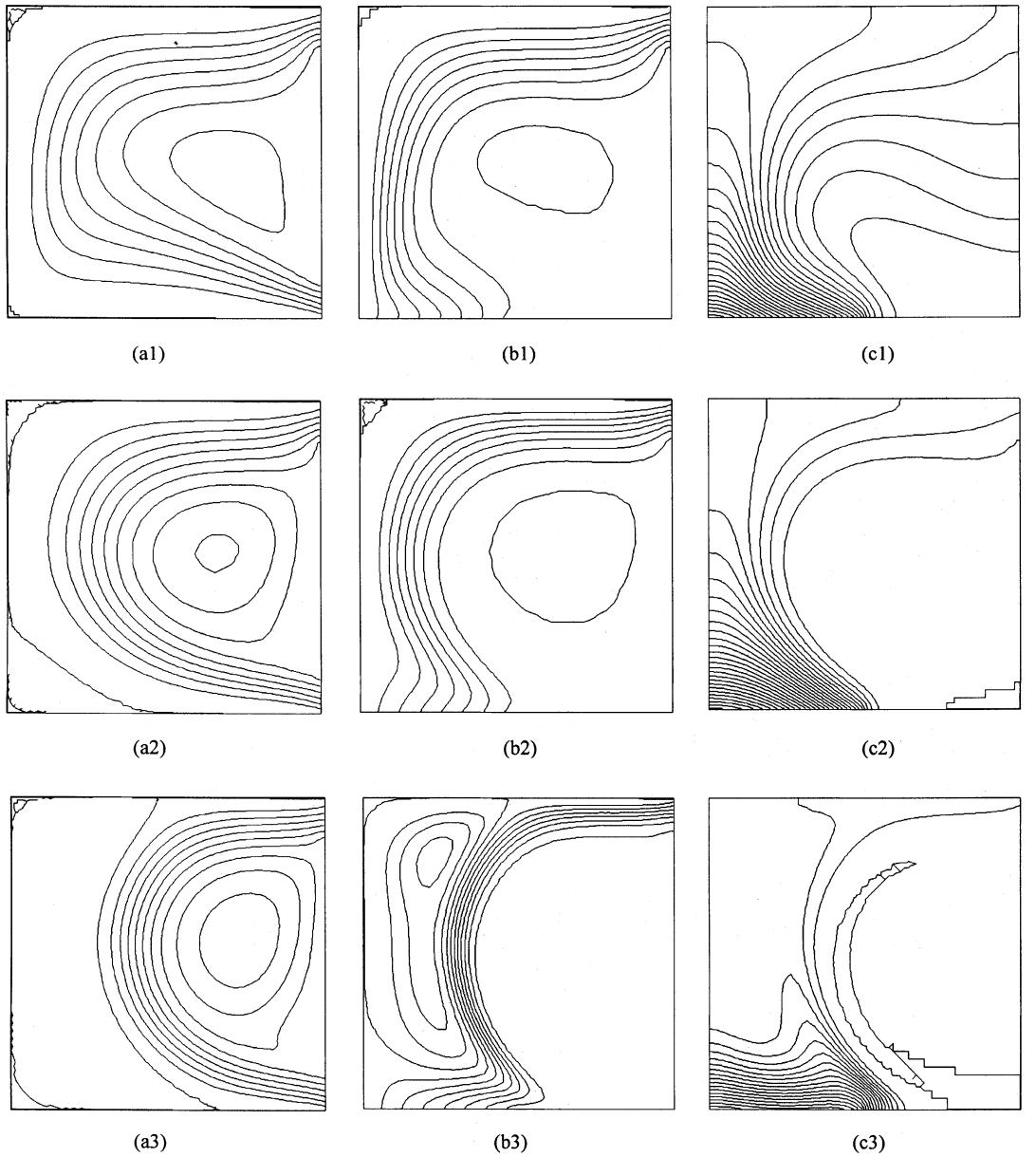

Fig. 3. Streamline (a), heatline (b) and isotherm (c) contours at $Gr = 10^5$ for different Gr/Re^2: (1) $Gr/Re^2 = 10$; (2) $Gr/Re^2 = 1$; (3) $Gr/Re^2 = 0.1$.

4.1. Effects of Gr and Gr/Re^2

Figs. 2–4 show the results at different Grashof number, i.e., $Gr = 10^4$–10^6. Note that the case of $Gr = 10^3$ is much similar to the case of $Gr = 10^4$.

For the case of $Gr = 10^4$, shown in Fig. 2, the heat source is relatively weak, with small heat flux on the surface. The relative magnitude Gr/Re^2 varies from the higher value $Gr/Re^2 = 1$ to the lower value $Gr/Re^2 = 0.01$, that is to say, the strength of the external forced flow, expressed by $Re/\sqrt{Gr}$, is enhanced gradually. When $Gr/Re^2 = 1$ or $Re = 100$, the forced cold flow is too weak, as compared with the buoyancy force. As seen from the streamlines, no recirculating flow occurs in the

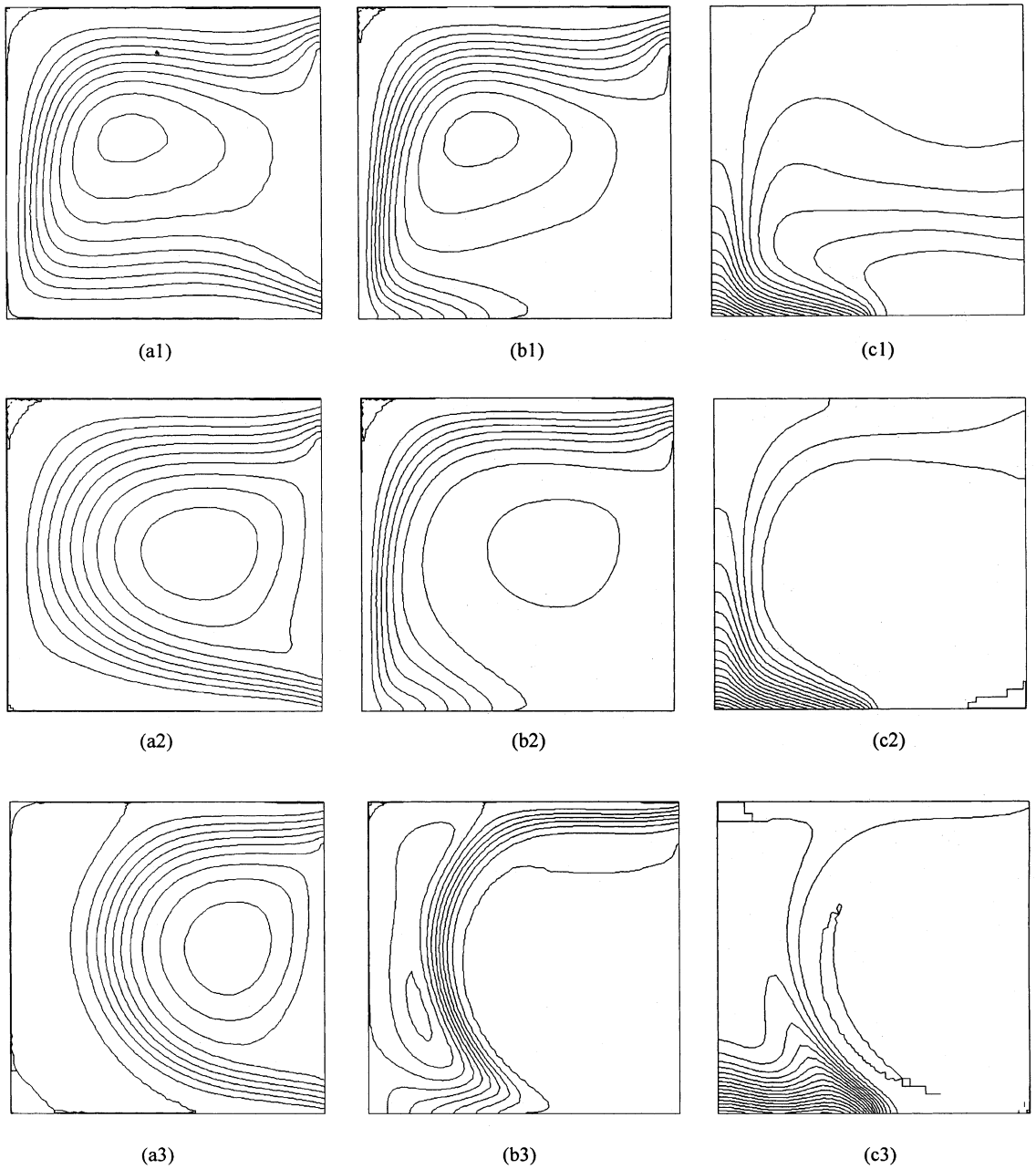

Fig. 4. Streamline (a), heatline (b) and isotherm (c) contours at $Gr = 10^6$ for different Gr/Re^2: (1) $Gr/Re^2 = 100$; (2) $Gr/Re^2 = 10$; (3) $Gr/Re^2 = 1$.

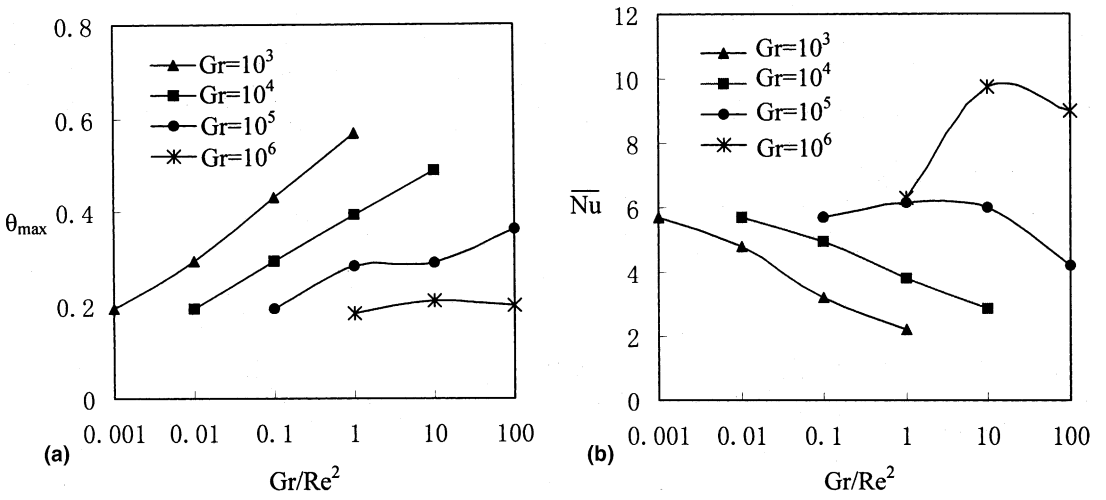

Fig. 5. Variations of the maximum temperature θ_{max} (a) and the average Nusselt number $\overline{Nu}$ (b) on the heat source surface.

working zone. Heatlines reveal that the heat is transferred from the source to a large portion of the room mainly by diffusion, which leads to a high temperature distribution of the whole room, as indicated by isotherm plot. Therefore, the IAQ of the working zone is poor when the external forced flow is too weak.

When the ratio Gr/Re^2 decreases to 0.1, the external forced cold flow becomes stronger. The streamlines illustrate the large recirculating cells appearing in the working zone. Heatline plot shows that the heat dissipated by the heat source is almost fully conveyed by the forced flow. The heat transfer is transported by the external forced cold flow, which acts an effect as isolating the heat, leaving the recirculating airflow in the working zone not infected by the heat source, which leads to a low air temperature distribution there as shown in isotherms. As a result, the IAQ of the working zone is better.

As Gr/Re^2 decreases further, to 0.01, the external forced cold flow is strong enough, but the buoyancy force generated by the heat source has also been strengthened with the increasing forced flow. As a result, the heat dissipated by the source cannot be fully conveyed by the external forced cold flow. It is seen in the heatlines that some amount of heat emitted by the heat source is left in the left close part of the room, while the remaining large amount of heat is vented out by the external forced flow. Likewise, the recirculting airflow in the working zone is fresh and cold, resulting in a higher IAQ.

Above basic phenomena observed in the case of $Gr = 10^4$ are also witnessed in the following cases of $Gr = 10^5$ and $Gr = 10^6$, as shown in Figs. 3 and 4. However, for keeping the Reynolds number invariant, the increasing value of Grashof number means the external forced flow being decreased, which gives rise to some important characteristics. The area affected by the forced flow is enlarged, as seen by streamlines. With the strengthen decreasing, the forced flow approaches closer to the opposite wall. As driven by the external forced flow, the system heat path moves nearer to the walls. The relatively weak forced flow cannot fully isolate the heat emitted by the heat source. As shown by heatlines, there are some recirculating heatlines arising in the working zone. However, this can be eliminated by increasing the forced flow, as shown in Figs. 3(3) and 4(3). It is worth noting that there is another change, occurring in the case of $Gr = 10^6$ and $Gr/Re^2 = 1$ where both the natural and the forced convection are strong, such that some heatlines recirculating just above the heat source, which is harmful to the heat dissipation rate as detailed in the following.

Fig. 5 plots the variations of the maximum temperature, θ_{max}, and the average Nusselt number, $\overline{Nu}$, in terms of the governing parameters, Gr and Gr/Re^2. It is observed that, for the same Grashof number or the heat source keeping constant, a decrease of the ratio Gr/Re^2 or an equivalent increase of the external forced flow, would decrease the temperature on the surface of the heat source, resulting in increasing the Nusselt number. The trend, however, is weaker for the higher Gr. Therefore, strengthening external forced flow would be much effective to eject the heat when the heat source is not very strong, but it does not work well when the heat source is strong enough. Taking $Gr = 10^6$ as an example, the maximum temperature on the heat source surface is not sensitive to increasing external forced flow or decreasing Gr/Re^2, but the average Nusselt number is largely decreased. This is due to the fact that some heat accumulating above the heat source (as indicated by heatlines) would inhibit the heat release rate.

4.2. Effects of the location of the outlet

Fig. 6 presents the results at $Gr = 10^4$ and $Gr/Re^2 = 0.1$ for different outlet location. It is found that, in all cases, the forced cold flow can control the heat source effectively, protecting the working zone from being contaminated by the heat source. But noticeable differences exist in their fluid and heat flow patterns. Heatlines imply that the nearer the outlet is from the heat source, the smaller the area affected, or in other words, the more effective it is to sweep out the heat, which resulting in lower temperature and higher Nusselt number on the surface of the heat source. Therefore, in order to obtain the best cooling effect of the heater and the lowest impact on other devices in the cavity, the outlet should be located on the nearest position to the

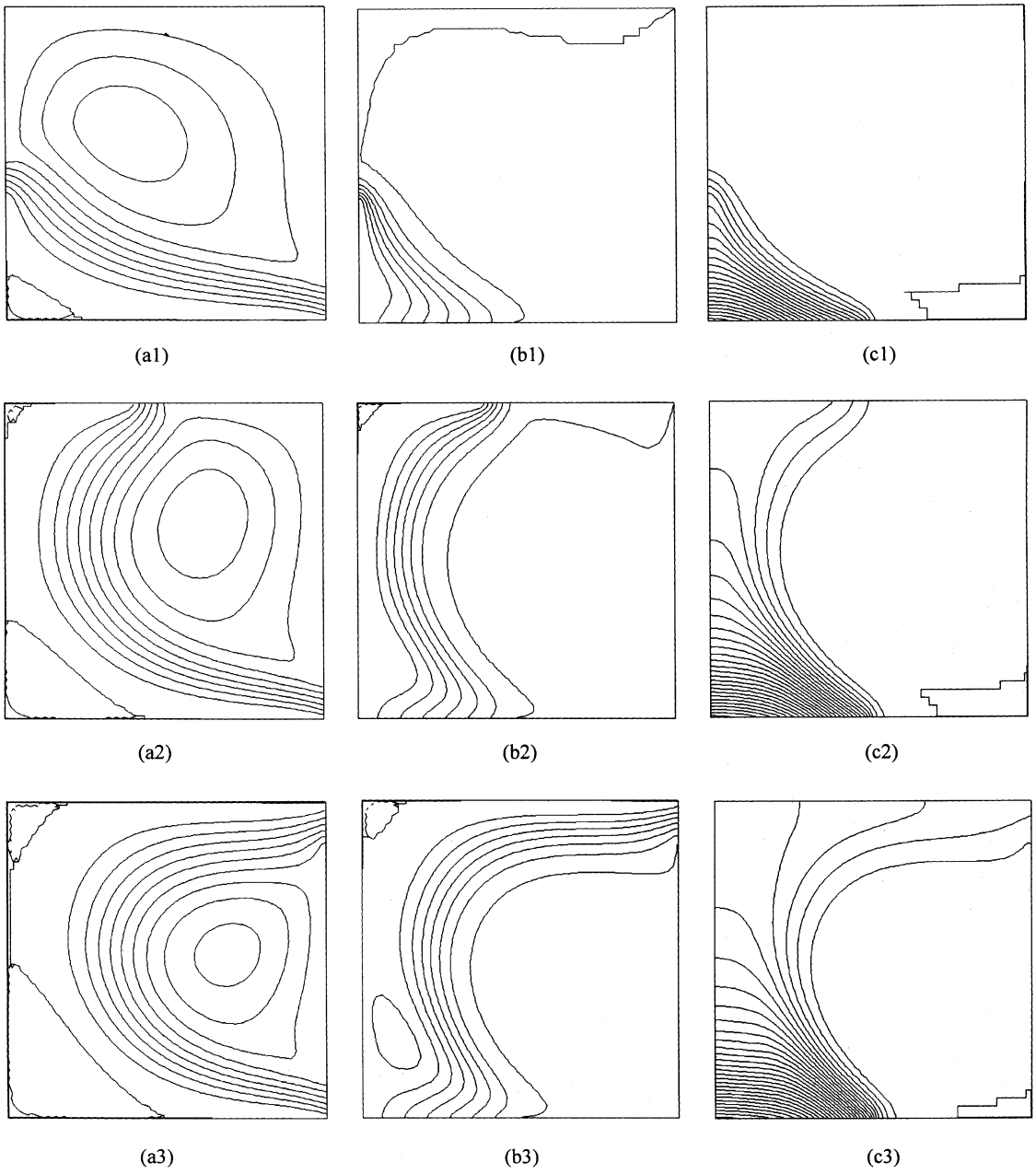

Fig. 6. Streamline (a), heatline (b) and isotherm (c) contours at $Gr = 10^4$ and $Gr/Re^2 = 0.1$ for different outlet position: (1) at left wall; (2) at top wall; (3) at right wall.

heat source, as it is done in the thermal management of electronic devices [10]. The recirculating flow in the work zone may be very weak, when the outlet is mounted on the opposite sidewall, as indicated by the sparse lines, which is not comfortable for the people working there. If outlet is on the same side of inlet, as the third case, the fluid flow is strong, and the temperature is low as well, which are beneficial to achieve a high IAQ for people in the working zone.

4.3. Results of the traditional ventilation

To illustrate the inefficiency of the traditional air-conditioning system, Fig. 7 presents the simulated

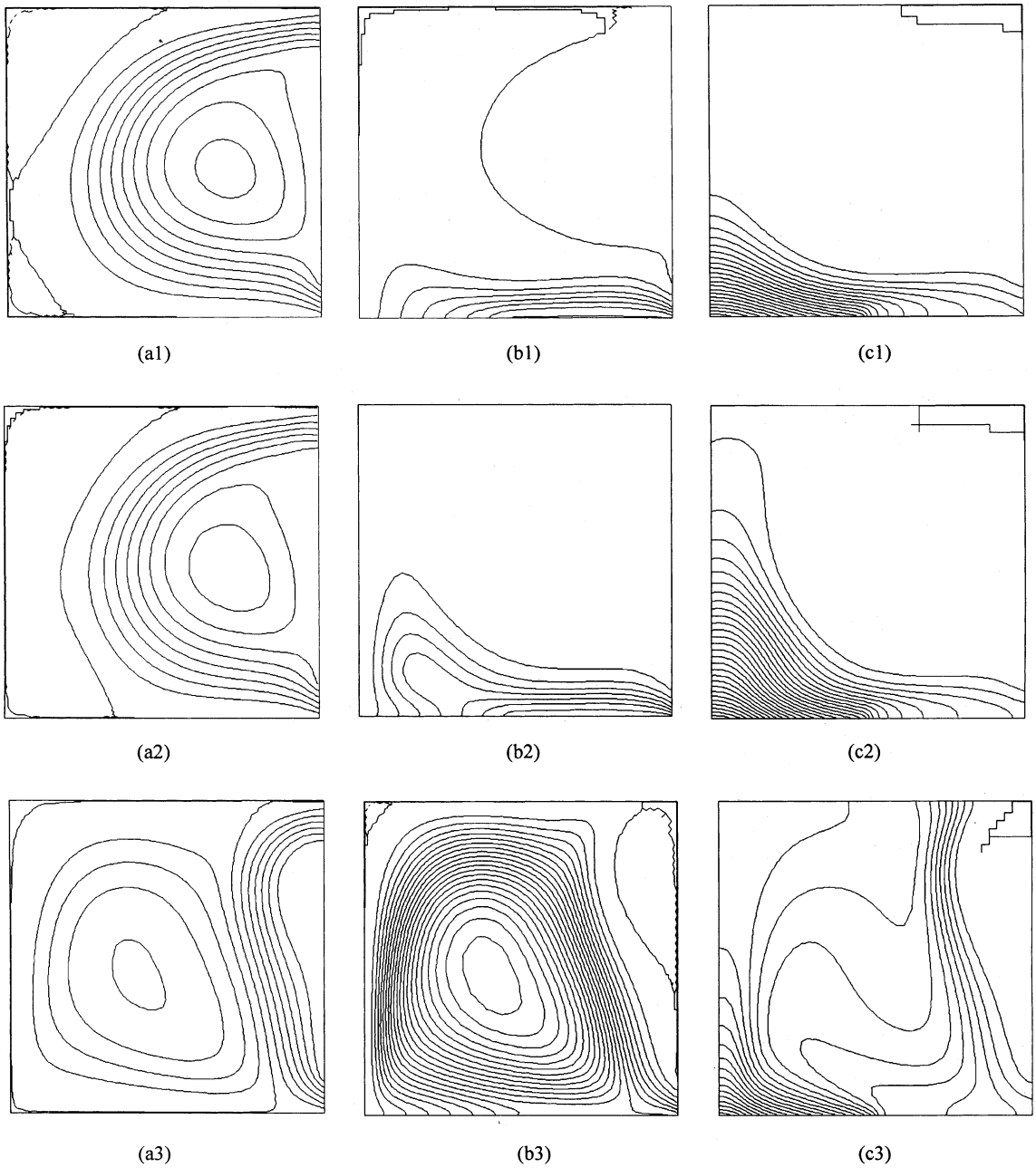

Fig. 7. Streamline (a), heatline (b) and isotherm (c) contours for inverse buoyancy and forced convection effect: (1) $Gr = 10^4$, $Gr/Re^2 = 0.1$; (2) $Gr = 10^5, Gr/Re^2 = 1$ (3) $Gr = 10^6, Gr/Re^2 = 10$.

results at different Grashof number, $Gr = 10^4$–10^6, for $Re = \sqrt{10} \times 100$. When the heat source is not very strong, at low value of Grashof number ($Gr \leqslant 10^5$), the traditional ventilation can still provide a suitable airflow environment in the working zone, as seen from the streamline pattern. But the thermal environment is worse, for the working area occupied by the stuff is infected by the heat source. Heatlines visualize that the heat transport path starts from the source, travels through the working zone and finally releases at the outlet. Once the heat source is strong enough, such as $Gr = 10^6$, the external forced cold flow cannot control the heat transport process, leading to the heat spread all over the domain. Apart from the phenomena above, it was found that the solution by the traditional ventilation is very delicate, i.e., the steady solution cast in a more narrower range of Reynolds number than that listed in Table 2, which means that the heat source is easily out of control of the external forced cold flow. To make a conclusion, the traditional ventilation system cannot provide a comfortable environment for occupants in the working zone, in the presence of the heat source. However, the displacement ventilation can ensure a higher IAQ and is therefore a desired air-conditioning system.

5. Conclusions

The method of streamline and heatline is extended to visualize the fluid flow and heat transfer for mixed convection. A two-dimensional, steady, laminar displacement ventilation model has been studied. The following conclusions are obtained:

1. The interaction between the buoyancy driven natural convection and the forced convection has important impact on the goal of ventilation effectiveness. The resulting heat and fluid flow structures are governed by two non-dimensional parameters Gr and Gr/Re^2.
2. Results for different outlet locations show that the nearer the outlet is from the heat source, the more effective it is to vent heat generated by the source, but the worser the in-door air quality (IAQ) is in the working area. To optimize the IAQ with the heat release effectiveness, the best position for the outlet will be on the same side of the inlet.
3. In the presence of the heat source in office, the traditional air-conditioning system cannot provide a healthy and comfortable working environment, but the displacement ventilation system works well.

References

[1] Q.-H. Deng, G.-F. Tang, Numerical visualization of mass and heat transport for conjugate natural convection/heat conduction by streamline and heatline, Int. J. Heat Mass Transfer 45 (2002) 2373–2385.
[2] X. Yuan, Q. Chen, L.R. Glicksman, A critical review of displacement ventilation, ASHRAE Trans. 104 (1998) 78–90.
[3] D. Blay, Convective phenomena involved in a displacement ventilation system, in: Indoor Air '96, 1996.
[4] ASHRAE Standard 62-1989, Ventilation for acceptable indoor air quality, Atlanta, GA, ASHRAE 1989.
[5] C. Collett, J. Ross, E. Sterling, Quality assurance strategies for investigating IAQ problems, ASHRAE J. 36 (1994) 42–51.
[6] P. Wargocki, D.P. Wyon, Y.K. Baik, et al., Perceived air quality, sick building syndrome (SBS) symptoms and productivity in an office with two different pollution loads, Indoor Air 9 (1999) 165–179.
[7] H.G. Lorsch, O.A. Abdou, The impact of the building indoor environment on occupant productivity, part I: recent studies, measures and costs, ASHRAE Trans. 100 (1994) 741–749.
[8] M. Sandberg, C. Blomguist, Displacement ventilation systems in office rooms, ASHRAE Trans. 95 (1989).
[9] E. Mundt, The performance of displacement ventilation system, PhD thesis, Royal Institute of Technology, Sweden, 1996.
[10] E. Papanicolaon, Y. Jaluria, Mixed convection from a isolated heat source in a rectangular enclosure, Numer. Heat Transfer, Part A 18 (1990) 427–461.